Investigations on the Influence of Temperature and Concentration on Solar Cell Performances

Henning Helmers, Michael Schachtner, Andreas W. Bett

Fraunhofer ISE, Heidenhofstr. 2, 79110 Freiburg, Germany

Abstract: In this study, the individual subcells made of $Ga_{0.50}In_{0.50}P$, $Ga_{0.99}In_{0.01}As$ and Ge of a lattice-matched triple-junction solar cell are investigated. Comprehensive measurements of the three corresponding component cells, which are optically equivalent to the triple-junction stack but electrically equivalent to a single subcells within the stack, are performed over a wide range of operating conditions. The investigated temperature range is 5 to 170 °C; the concentration ratio is varied from 1 to 3000. Measurement results are presented and an analytical model is used to describe the temperature and irradiance dependence of the open circuit voltage $V_{OC}(T,C)$.

Keywords: Characterization; component cells; CPV; CPVT; multi-junction; open circuit voltage; temperature dependence; temperature coefficient; space.
PACS: 73.61.Ey; 88.40.hj; 88.40.jp;

INTRODUCTION

Multi-junction solar cells are usually characterized at standard testing conditions (STC) at a temperature of 25 °C and an irradiance of 1000 W/m². Opposed to that, in real applications in terrestrial concentrator systems and also in some space missions, the operating conditions differ strongly from these conditions. In passively cooled CPV systems the operating cell temperature can reach 80 °C [1, 2] and typical concentration ratios range from 300 to 1000. Moreover, in actively cooled concentrating photovoltaic and thermal (CPVT) systems with central receiver, even higher operating temperatures >100 °C are desirable [3], because then the value of the generated heat increases [4] and sophisticated heat applications, such as industrial process heating, solar cooling [5] or solar desalination [6], become feasible. Also in space missions close to the sun high temperature and high irradiance conditions occur. E.g., in the Bepi Colombo mission to Mercury the projected cell temperature is 230 °C at an irradiance of 11 solar constants [7]; in the Solar Probe Plus mission to the sun, the projected operation conditions are 120 °C at a solar intensity of 250 suns [8].

Existing literature covers analyses of the temperature dependence of multi-junction solar cells, party also with respect to varying irradiance (compare e.g. Refs. 9 through 15). However, analysis of the multi-junction stack as a whole provides no, or only indirect, information about the individual behavior of the subcells within the stack. For that reason, in this work component solar cells were investigated to analyze the influence of temperature T and concentration C on the performance of the subcells of a lattice-matched triple-junction solar cell.

The results are analyzed in light of the question at which temperature the open circuit voltage V_{OC} of the respective subcells vanishes. Therefore, an analytical expression is used to extrapolate $V_{OC}(T,C)$ data.

OPEN CIRCUIT VOLTAGE MODEL

In the following, an analytical expression of the open circuit voltage V_{OC} as a function of temperature T and concentration ratio C is derived.[1]

Under concentration bulk recombination dominates the recombination processes within the solar cell and a one diode model is sufficient to describe the current-voltage characteristics. With $J_{ph}=CJ_{SC}^{1x} \gg J_0$ it follows:

$$V_{OC} = \frac{kT}{q} \ln\left\{\frac{CJ_{SC}^{1x}}{J_0}\right\}, \tag{1}$$

with Boltzmann constant k, elementary charge q, photo-generated current density J_{ph}, short circuit current density at one sun condition J_{SC}^{1x}, and recombination current density J_0.

For the assumed dominating bulk recombination, J_0 takes the form [16]:

$$J_0 = n_i^2 q\left(\frac{L_e}{N_A\tau_e} + \frac{L_h}{N_D\tau_h}\right), \tag{2}$$

where n_i is the intrinsic carrier concentration, N_A and N_D are the densities of acceptor and donor atoms in base and emitter, respectively, and L and τ are the

[1] Note that a similar treatment was presented by Nishioka et al. to derive an expression for dV_{OC}/dT [10].

lifetime and the diffusion length of the minority carriers, respectively. The indices e and h denote the respective types of minority carriers, i.e. electrons in p-type and holes in n-type material.

Assuming $L_e/(N_A\tau_e) \gg L_h/(N_D\tau_h)$ for n^+/p material, Eq. (2) reduces to

$$J_0 = n_i^2 \frac{q}{N_A} \frac{L_e}{\tau_e} . \quad (3)$$

In Eq. (3), q and N_A are independent of temperature, whereas n_i, L and τ in general are temperature dependent.

From the fundamental law of mass action, the temperature dependence of the intrinsic carrier concentration n_i derives to [16]:

$$n_i(T)^2 = N_C N_V \exp\left\{-\frac{E_g(T)}{kT}\right\}, \quad (4)$$

with the effective densities of states N_C and N_V of conduction and valence band, and the temperature dependent band gap $E_g(T)$, which can be well described by an expression derived by Varshni [17]:

$$E_g(T) = E_g(0) - \frac{\alpha T^2}{T+\beta}, \quad (5)$$

where $E_g(0)$, α and β are material constants. Note that for many specific compositions of ternary compound semiconductors, these constants are not available. In this case, a bowing formalism between the band gaps of the related binary materials is applicable as described by Vurgaftman et al. [18].

Equating N_C and N_V in Eq. (4) yields an explicit expression of the temperature dependence of $n_i(T)$:

$$n_i(T)^2 = 4\left(\frac{2\pi k\sqrt{m_e^* m_h^*}}{h^2}\right) \cdot T^3 \exp\left\{-\frac{E_g(T)}{kT}\right\}, (6)$$

where h is the Planck constant and $m^*_{e/h}$ are the effective masses of electrons and holes, respectively.

The temperature behavior of the diffusion length and lifetime is more complex and not well understood so far. Sze [16] proposed a power-law temperature dependence that has been applied in earlier works [10, 11, 14]. With γ being the power-law exponent of the temperature dependence of the quotient of diffusion constant D and minority carrier lifetime τ, it takes the form:

$$\frac{L}{\tau} = \left(\frac{D}{\tau}\right)^{1/2} \propto T^{\gamma/2} . \quad (7)$$

Combination of Eqs. (3) through (7) and separation of the temperature dependence of the parameters from its values at 300 K yield an expression of the temperature dependence of the recombination current $J_0(T)$:

$$J_0(T) = \frac{q}{N_A} N_C^{300\text{K}} N_V^{300\text{K}} \frac{L^{300\text{K}}}{\tau^{300\text{K}}} \times \left(\frac{T}{300\text{K}}\right)^{3+\frac{\gamma}{2}} \exp\left\{-\frac{E_g(T)}{kT}\right\} . \quad (8)$$

In general, the intrinsic semiconductor properties $L^{300\text{K}}$ and $\tau^{300\text{K}}$ as well as their temperature dependence γ depend on the magnitude of the irradiance. Therefore, the expression in Eq. (8) represents an implicit function of concentration ratio C in these parameters.

Finally, substitution of J_0 in Eq. (1) by the expression in Eq. (8) yields the desired expression for the open circuit voltage as a function of temperature and concentration ratio. With the thermal voltage $V_T \equiv kT/q$, the band gap voltage $V_g \equiv E_g/q$, and the material constant $M \equiv qN_C^{300\text{K}} N_V^{300\text{K}}/N_A$, it takes the form:

$$V_{OC}(T,C) = V_g(T) - V_T\left[\ln\left\{M\frac{L^{300\text{K}}}{\tau^{300\text{K}}}\right\} + \left(3+\frac{\gamma}{2}\right)\ln\left(\frac{T}{300\text{K}}\right)\right] + V_T \ln\left\{C \cdot J_{SC}^{1x}(T)\right\} . \quad (9)$$

To first order, the V_{OC} can be approximated by a linear function of temperature. Deviations from linearity occur from the quadratic term in the band gap voltage (compare Eq. (5)), from the second term in square brackets that comprises the temperature dependences of the effective densities of states of conduction and valence band, diffusion length and lifetime, and from the implicit temperature dependence of the short circuit current density $J_{SC}^{1x}(T)$. Regarding concentration ratio, Eq. (9) illustrates that the open circuit voltage increases logarithmically as the concentration ratio increases.

MEASUREMENT

The three subcells of the lattice-matched triple-junction solar cell (i.e. $Ga_{0.50}In_{0.50}P$, $Ga_{0.99}In_{0.01}As$, Ge) were investigated using corresponding component solar cells. These devices are optically equivalent to the triple-junction structure, but feature only one active p-n-junction and are, thus, electrically equivalent to an individual subcell within the multi-junction stack.

A Peltier controlled set-up was used for temperature control of the test samples from 5 to 170 °C. During the 5 °C measurement a nitrogen shower was used to prevent water condensation from the laboratory atmosphere. The external quantum efficiencies and the one-sun I-V curves under

1000 W/m², AM1.5d, were measured over the whole temperature range using a grating monochromator and a multi-source sun simulator, respectively. Afterwards, temperature dependent measurements under concentration up to C=3000 were performed using a flash sun simulator.

RESULTS

In the following, the one-sun I-V curves and an analysis of the measured open circuit voltages are presented. A comprehensive presentation and analysis of the measurement data can additionally be found in Ref. 19, including a detailed analysis of the Ge subcell behavior at high temperatures and a derivation of the limit temperature where V_{OC} of the subcells vanish.

I-V Curves

The temperature dependent one-sun I-V curves of the $Ga_{0.50}In_{0.50}P$, $Ga_{0.99}In_{0.01}As$, and Ge cells are shown in Figure 1. As can be observed in the graph, with increasing temperature the open circuit voltage decreases significantly, whereas the short circuit current density increases only slightly. The temperature coefficients, defined as the slope of a linear fit through the values plotted against temperature, are listed in Table 1.

Analysis of the short circuit current densities of the component cells yields information about the quality of current matching of the subcells if they would form a multi-junction stack. At 25 °C the $Ga_{0.50}In_{0.50}P$ cell is current limiting, while the $Ga_{0.99}In_{0.01}As$ shows a slight excess current of 1.3 %. As the temperature rises, the current of both subcells increases. However, the increase is larger for the $Ga_{0.50}In_{0.50}P$ cell. Consequently, the current limitation shifts to the $Ga_{0.99}In_{0.01}As$ cell. At 170 °C the current matching situation is inverted and the $Ga_{0.50}In_{0.50}P$ shows a slight excess current of 1.2 % compared with the current limiting $Ga_{0.99}In_{0.01}As$ cell. Thus, the top and middle subcells are well current matched over the whole investigated temperature range. As to the Ge bottom subcell, it features an excess current of 60.1 to 63.3 % compared with the limiting current over the entire temperature range.

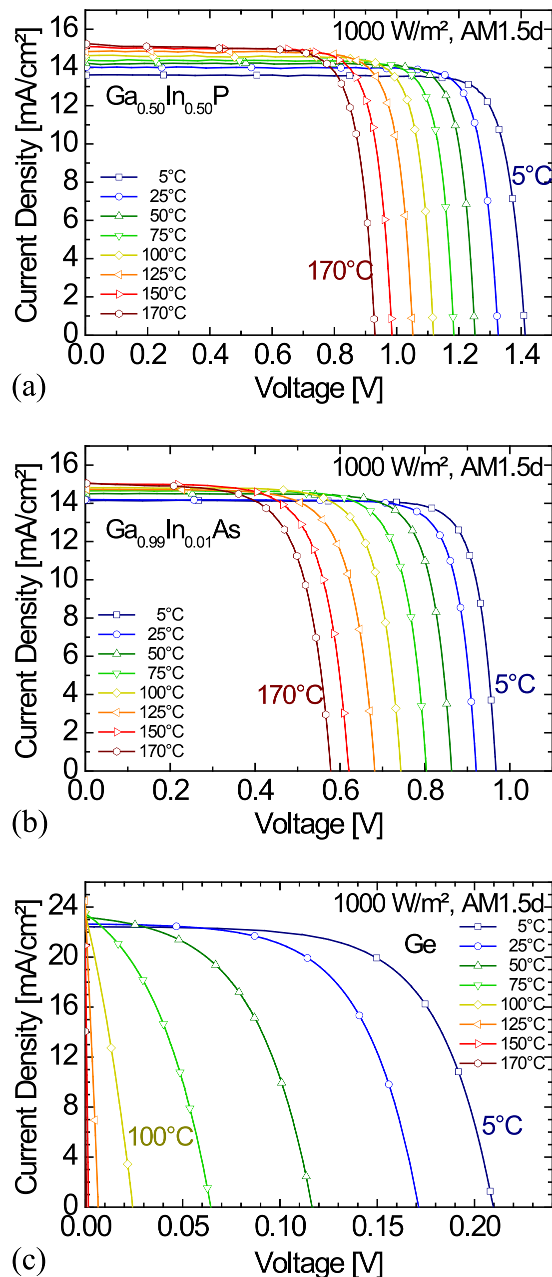

FIGURE 1. Temperature dependent I-V curves of the $Ga_{0.50}In_{0.50}P$ (a), $Ga_{0.99}In_{0.01}As$ (b), and Ge (c) component cells under one-sun conditions (1000 W/m², AM1.5d).

TABLE 1. Absolute and relative temperature coefficients, TC_{abs} and TC_{rel}, of the short circuit current densities J_{SC} and the open circuit voltages V_{OC} of the three component cells determined under one sun illumination conditions. The absolute value is determined from the slope of a linear fit of the values plotted against temperature; the relative value is calculated by division by the corresponding value at 25 °C.

Material	$TC_{abs}(J_{SC})$ [µA/cm²/K]	$TC_{rel}(J_{SC})$ [%/K]	$TC_{abs}(V_{OC})$ [mV/K]	$TC_{rel}(V_{OC})$ [%/K]
$Ga_{0.50}In_{0.50}P$	9.3	0.07	-2.8	-0.21
$Ga_{0.99}In_{0.01}As$	5.6	0.04	-2.4	-0.26
Ge	6.7	0.03	-2.1	-1.22

Open Circuit Voltage

Figure 2 shows the measured open circuit voltages of the three component cells as a function of temperature for varying concentration ratios.

The measured data was fitted to the analytical $V_{OC}(T,C)$ model after Eq. (9) for each concentration (solid lines in Figure 2). Since the model is not able to describe the saturation region close to zero, these values have been neglected for the fit procedure. L^{300K}/τ^{300K} and γ constitute the two fit parameters, the other quantities are either known (base-doping N_A), measured (one-sun current density J_{SC}^{1x},) or taken from literature (effective densities of states at 300 K, N_C^{300K} and N_V^{300K}, band gap E_g) from Refs. 18, 20, 21. As can be seen in Figure 2, the fits well describe the measured data. Consequently, it is concluded that the presented model well describes the temperature and irradiance dependence of V_{OC}.

As observed in Figure 2c, the limit temperature T_{limit}, defined as the temperature where V_{OC} vanishes, of the Ge subcell is lower than potential operating temperatures in particular concentrator and space applications. In this case, a Ge-less dual-junction device becomes comparable with the triple-junction structure (see Ref. 19 for a more detailed discussion).

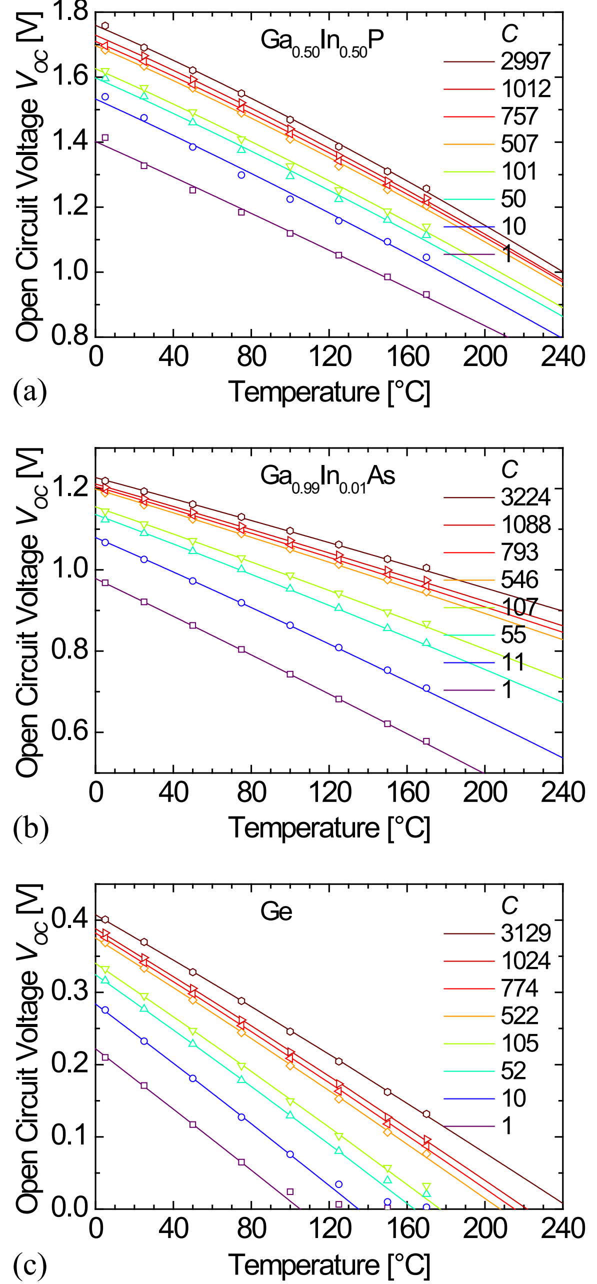

FIGURE 2. Open circuit voltages of the $Ga_{0.50}In_{0.50}P$ (a), $Ga_{0.99}In_{0.01}As$ (b), and Ge (c) component cell as a function of temperature for varying concentration ratio. The symbols represent the measured data. The lines represent corresponding fits after Eq. (9), where L^{300K}/τ^{300K} and γ are the two fit parameters.

CONCLUSION

A comprehensive study of the behavior of the three subcells of the lattice-matched triple-junction solar cell under varying temperature and concentration was carried out. The measurements cover a large range of operating conditions, namely temperatures from 5 to 170 °C and concentration ratios from 1 to 3000. Measurement results were presented. An analytical model of the open circuit voltage as a function of temperature and concentration ratio was derived and used to describe the measurement data. At high temperature the open circuit voltage vanishes. The corresponding limit temperatures can be quantified by extrapolation of the measurement data using the model. It has been shown that for particular high temperature conditions, a Ge-less dual-junction device can become comparable to the triple-junction structure, because the Ge subcell ceases to contribute to the power output of the multi-junction stack at high temperature.

ACKNOWLEDGMENTS

The authors thank A. Bühl and E. Fehrenbacher for measurements and S. Gamisch for support. Additional thanks to S. Philipps for organizational support.

H. Helmers gratefully acknowledges the scholarship support of the German Federal Environmental Foundation (DBU). This work was partly funded by the Federal Ministry for the Environment, Nature Conservation and Nuclear Safety (BMU) under the "KoMGen" project (#0327567A).

This work was partly supported by the European Commision under the project NGCPV with Grant agreement no. 283798. The authors are responsible for the content of this work.

REFERENCES

1. J. Jaus, R. Hue, M. Wiesenfahrt, G. Peharz, A.W. Bett, in *Proc. 23rd EU PVSEC*, Valencia, Spain, 2008, pp. 832-836. DOI: 10.4229/23rdEUPVSEC2008-1DV.3.23
2. M. Wiesenfahrt, H. Kraus, S. Gamisch, A.W. Bett, in *Proc. CPV-9*, Miyazaki, Japan, 2013.
3. H. Helmers, A.W. Bett, J. Parisi, C. Agert, *Prog. Photovolt. Res. Appl.* (2012). DOI: 10.1002/pip.2287
4. J. S. Coventry and K. Lovegrove, *Sol. Energy* **75**(1), 63-72 (2003). DOI: 10.1016/S0038-092X(03)00231-7
5. G. Mittelman, A. Kribus, A. Dayan, *Energy Conv. Manag.* **48**(9), 2481-2490 (2007). DOI: 10.1016/j.enconman.2007.04.004
6. G. Mittelman, A. Kribus, O. Mouchtar, A. Dayan, *Sol. Energy* **83**(8), 1322-1334 (2009). DOI: 10.1016/j.solener.2009.04.003
7. C.G. Zimmermann, C. Nömayr, M. Kolb, A. Caon, in *Proc. 37th IEEE PVSC*. Seattle, USA, 2011. pp. 3713-3718. DOI: 10.1109/PVSC.2011.6185957
8. NASA, Report No. NASA/TM—2008–214161, 2008.
9. K. Nishioka, T. Takamoto, T. Agui, M. Kaneiwa, Y. Uraoka, T. Fuyuki, *Sol. Energy Mater. Sol. Cells* **85**(3), 429-436 (2005). DOI: 10.1016/j.solmat.2004.05.008
10. K. Nishioka, T. Takamoto, T. Agui, M. Kaneiwa, Y. Uraoka, T. Fuyuki, *Sol. Energy Mater. Sol. Cells* **90**, 57-67 (2006). DOI: 10.1016/j.solmat.2005.01.011
11. G.S. Kinsey, P. Hebert, K.E. Barbour, D.D. Krut, H.L. Cotal, R.A. Sherif, *Prog. Photovolt. Res. Appl.* **16**(6), 503-508 (2008). DOI: 10.1002/pip.834
12. A. Braun, B. Hirsch, A. Vossier, E.A. Katz, J.M. Gordon, *Prog. Photovolt. Res. Appl.* **21**(2), 202–208 (2013). DOI: 10.1002/pip.1179.
13. G. Siefer, A.W. Bett, *Prog. Photovolt. Res. Appl.* (2012). DOI: 10.1002/pip.2285
14. W. Bagienski, G.S. Kinsey, M. Liu, A. Nayak, V. Garboushian, in *Proc. CPV-8*, Toledo, Spain, 2012, AIP 1477, pp. 148-151. DOI: 10.1063/1.4753855.
15. E.F. Fernandez, G. Siefer, M. Schachtner, A.J.G. Loureiro, P. Perez-Higueras, in *Proc. CPV-8*, Toledo, Spain, 2012, AIP 1477, pp. 189-193. DOI: 10.1063/1.4753865.
16. S.M. Sze, *Physics of Semiconductor Devices*, New York, USA: John Wiley and Sons, 1981.
17. Y.P. Varshni, *Physica* **34**(1), 149-154 (1967). DOI: 10.1016/0031-8914(67)90062-6
18. I. Vurgaftman, J.R. Meyer, L.R. Ram-Mohan, *J. Appl. Phys.* **89**(11), 5815-5875 (2001). DOI: 10.1063/1.1368156
19. H. Helmers, M. Schachtner, A.W. Bett, *Sol. Energy Mat. Sol. Cells* (2013). DOI: 10.1016/j.solmat.2013.03.039
20. M. Levinshtein, S. Rumyantsev, M. Shur, in *Handbook Series on Semiconductor Parameters* (World Scientific Publishing, Singapore, 1996), Vol. 1: *Si, Ge, C (Diamond), GaAs, GaP, GaSb, InAs, InP, InSb.*
21. M. Levinshtein, S. Rumyantsev, M. Shur, in *Handbook Series on Semiconductor Parameters* (World Scientific Publishing, Singapore, 1999), Vol. 2: *Ternary and Quaternary III-V Compounds.*